

Numerical modeling of the aging effects of RC shear walls strengthened by CFRP plates: A comparison of results from different “code type” models

Redha Yeghne^{*1,2}, Hicham Zakaria Guerrouj^{1b}, Lemya Hanifi Hachemi Amar^{1b},
Sid Ahmed Meftah^{3a}, Samir Benyoucef^{2a}, Abdelouahed Tounsi^{2,3a} and El Abbas Adda Bedia^{2a}

¹Department of Civil Engineering and Hydraulics, University Dr. Tahar Moulay, PBox 138 City En-Nasr 20000 Saida, Algeria

²Laboratory of Materials and Hydrology (LM&H), University Djillali Liabès, Sidi Bel Abbès, Algeria

³Laboratory of Structures et Matériaux Avancés dans le Génie Civil et Travaux Publics (SMAGCTP), University Djillali Liabès, Sidi Bel Abbès, Algeria

(Received August 1, 2016, Revised February 1, 2017, Accepted February 12, 2017)

Abstract. Creep and shrinkage are the main types of volume change with time in concrete. These changes cause deflection, cracking and stresses that affect durability, serviceability, long-term reliability and structural integrity of civil engineering infrastructure. Although laboratory test may be undertaken to determine the deformation properties of concrete, these are time-consuming, often expensive and generally not a practical option. Therefore, relatively simple empirically design code models are relied to predict the creep strain.

This paper reviews the accuracy of creep and shrinkage predictions of reinforced concrete (RC) shear walls structures strengthened with carbon fibre reinforced polymer (CFRP) plates, which is characterized by a widthwise varying fibre volume fraction. This review is yielded by three commonly used international “code type” models.

The assessed are the: CEB-FIP MC 90 model, ACI 209 model and Bazant & Baweja (B3) model. The time-dependent behavior was investigated to analyze their seismic behavior. In the numerical formulation, the adherents and the adhesives are all modelled as shear wall elements, using the mixed finite element method. Several tests were used to demonstrate the accuracy and effectiveness of the proposed method. Numerical results from the present analysis are presented to illustrate the significance of the time-dependency of the lateral displacements and eigenfrequencies modes.

Keywords: RC shear walls strengthened; CFRP plates; creep and shrinkage; finite element method; seismic behavior; numerical modeling

1. Introduction

In structural engineering, a shear wall is a structural system used to counter the effects of lateral loads acting on a structure. The concrete shear walls must resist to lateral loads due to earthquakes. However, structural damages and early code shortcomings threaten the efficiency of existing structural walls against earthquake.

The time-varying behavior of reinforced concrete structures under sustained service loads drawn the attention of engineers who were dealing with the problems of their design more than 60 years. The solution of structural problems involving creep and shrinkage phenomena in composite steel-concrete structures has been an important task of engineers since the first formulation of the mathematical model of linear viscoelasticity. The development of structural analysis procedures, based on the creep models, is of great interest for engineers who need to investigate the effects of creep and shrinkage on the concrete structures.

The time-dependent behavior of concrete structures due to their properties of shrinkage and creep may lead to cause excessive strain and stress redistribution (Al-Manasseer and Lam 2005). It's can lead to cracking caused by stresses developed in concrete (Chia *et al.* 2014). The redistribution of stresses and excessive strain, if not detected and treated properly, exerts a deterioration of concrete structures and even their collapse, resulting in economic and social costs (Almeida 2006).

Several techniques are currently available to repair and retrofit these shear walls structure with insufficient stiffness, strength and/or ductility. These techniques include the strengthening of existing shear walls by the application of shotcrete of ferrocement, filling in openings with reinforced concrete and masonry infills, and the addition of new shear walls (Chung *et al.* 2014).

Recently, new strengthening or rehabilitation techniques and materials of reinforced concrete structures have been developed, among them new products based on advanced composite materials known as fibre reinforced polymers (FRP) can be cited (Mini *et al.* 2014, Boukhezar *et al.* 2013, Wang *et al.* 2014, Yeghne^{et al.} 2009, Sakr *et al.* 2017). FRP materials benefit several advantages in material properties and performance compared to the older building materials, causing much interest in their use in civil engineering areas and to repair damaged structures

*Corresponding author, Ph.D.

E-mail: yeghne@reda2000@yahoo.fr

^aPh.D.

^bPh.D. Student

Table 1 Formulas for the modulus of elasticity at age for 28 days

Design code	Formula for E_c (MPa)
Eurocode 2	$E_{cm} = 22000(0,1 \cdot f_{cm})^{0,3}$
CEB-FIP Code Model	$E_{cm} = 9980\sqrt[3]{f_{cm}}$
ACI 318	$E_c = 4733\sqrt{f_{cm}}$

(Yeghnem et al. 2015).

An important issue in this study is the time-dependent analysis of seismic response of RC shear walls strengthened with composite sheets, having a sinusoidal distribution of fibres. A three shrinkage and creep predictions models have been used to study the behavior of concrete including their rheological properties. Those models are namely: CEB-FIP MC 90 model, ACI 209 model and Bazant & Baweja (B3) model.

2. Recommendations for modeling creep and shrinkage of concrete

The prediction of creep and shrinkage effects in concrete structures as well as effects of various relevant variables related to material properties, climate and member size are provided in detail in many code type models.

2.1 Shrinkage and creep prediction techniques

Designers typically use one of two code methods to estimate creep and shrinkage strain in concrete, i.e., either Eurocode 2 or ACI 318. Eurocode 2 is based on the CEB-FIP MC 90 model recommended by the Euro-International Committee, and ACI 318 is based on the ACI 209 model recommended by the American Concrete Institute (Meyerson et al. 2002). This chapter presents three shrinkage and creep predictions models, namely the CEB-FIP MC 90 model, ACI 209 model, and Bazant & Baweja (B3) model.

2.2 Modulus of elasticity

The modulus of elasticity is an input parameter to the creep compliance. It is defined as the tangent modulus of elasticity at the origin of the stress-strain diagram and can be estimated from the mean compressive cylinder strength and the concrete age. The tangent modulus E_c is approximately equal to the secant modulus E_{cm} of unloading which is usually measured in tests. Formulas according to some relevant design codes are shown in Table 1, where f_{cm} is the mean concrete cylinder compressive strength at the age of 28 days (MPa).

Besides the concrete strength, the elastic modulus depends also on the type of the aggregate, the curing conditions and the test method. The influences of these factors are largely responsible for the significant scatter which can be observed when experimental values of the modulus of elasticity are plotted against the concrete strength (Takács 2002). Test result of the elastic modulus is usually available for major structures but it is very rare that

at least a short-term creep test is carried out (Takács 2002).

2.3 CEB-FIP Model Code 1990 (MC 90)

The equations presented here were published in the final draft of the MC 90 (CEB-FIP MC 90 1991). The model is valid for normal density concrete with grade up to C80 and exposed to a mean relative humidity in the range of 40 to 100%. At the time when the code was prepared, very limited information on concrete with a characteristic strength higher than 50 MPa were available and therefore the models should be used with caution in that strength range.

The CEB-FIP MC 90 procedure computes the creep compliance by Eq. (1)

$$J(t, t_0) = \frac{1}{E_c(t_0)} + \frac{\Phi(t, t_0)}{E_c} \quad (1)$$

Where

$\Phi(t, t_0)$: the creep coefficient;

t_0 : the age of concrete at loading in days;

$E_c=1,1 \cdot E_{cm}$: the tangent modulus at the age of 28 days (MPa);

$E_c(t_0)$: the tangent modulus at the age of loading t_0 (MPa).

The creep coefficient is shown below

$$\Phi(t, t_0) = \Phi_0 \beta_c c(t - t_0) \quad (2)$$

Where

Φ_0 : the notional creep coefficient;

$\beta_c(t-t_0)$: the coefficient to describe the development of creep with time after loading. The notional creep coefficient can be determined by the following equations

$$\Phi_0 = \Phi_{RH} \beta(f_{cm}) \beta(t_0) \quad (3)$$

$$\Phi_{RH} = 1 + \frac{1 - RH/100}{0,1 \sqrt[3]{h_0}} \quad (4)$$

$$\beta(f_{cm}) = \frac{16,8}{\sqrt{f_{cm}}} \quad (5)$$

$$\beta(t_0) = \frac{1}{0,1 + t_0^{0,2}} \quad (6)$$

$$h_0 = \frac{2A_c}{u} \quad (7)$$

Where

RH : the relative humidity of the ambient environment, expressed in %;

h_0 : the notional size of the shear wall (mm);

A_c : the cross-sectional area of the shear wall (mm²);

U : the perimeter of member exposed to the atmosphere (mm).

The time development function for the creep coefficient is written as

$$\beta_c(t - t_0) = \left[\frac{t - t_0}{\beta_H + t - t_0} \right]^{0,3} \quad (8)$$

$$\beta_H = 1,5[1 + (0,012 \cdot RH)^{18}] h_0 + 250 \leq 1500 \quad (9)$$

The shrinkage strain is calculated by

$$\varepsilon_b^f(y) = \varepsilon_{cs}(t, t_s) = \varepsilon_{cs0} \beta_s s(t - t_s) \quad (10)$$

Where

ε_{cs0} : the notional shrinkage coefficient;

β_s : the time function to describe the development of shrinkage with time;

t_s : the age of concrete when drying begins in days.

The notional shrinkage coefficient can be estimated from

$$\varepsilon_{cs0} = \varepsilon_s(f_{cm}) \beta_{RH} \quad (11)$$

Where

$$\varepsilon_s(f_{cm}) = [160 + 10\beta_{sc}(9 - 0,1f_{cm})] \cdot 10^{-6} \quad (12)$$

$$\beta_{RH} = \begin{cases} -1,55 \cdot \left[1 - \left(\frac{RH}{100}\right)^3\right], & RH < \beta_{s1} \cdot 99\% \\ 0,25, & RH \geq \beta_{s1} \cdot 99\%, \end{cases} \quad (13)$$

Where β_{sc} is a coefficient which depends on the cement type, 4 for slowly hardening cement, 5 for normal and rapid hardening cement and 8 for rapid hardening high strength cement; factor β_{s1} was assumed equal to 1,0. RH in Eq. (13) should be not less than 40%.

The development of shrinkage with time is given by

$$\beta_s(t - t_s) = \sqrt{\frac{t - t_s}{0,035 \cdot h_0^2 + t - t_s}} \quad (14)$$

The influence of mean temperature other than 20°C can be also taken into account. With the decreasing temperature both the notional creep coefficient and the notional shrinkage coefficient are decreasing and their development with time are decelerated.

2.4 The 1999 update of the CEB-FIP MC1990

The models were published in the fib Bulletin (FIB 1999). The primary intention with the update was to improve the prediction models for high-strength concrete and further extend the validity of the models to high-performance concrete.

The updated creep model was in fact first published in Eurocode 2 (Eurocode 2 2001). It is closely related to the model in the MC 90 (CEB-FIP MC 90 1991), but three strength dependent coefficients were introduced into the original model. The extended model is valid for both normal strength concrete and high performance concrete up to concrete cylinder strength of 110 MPa. Three coefficients were introduced into the MC 90 model

$$\alpha_1 = \left(\frac{35}{f_{cm}}\right)^{0,7}; \alpha_2 = \left(\frac{35}{f_{cm}}\right)^{0,2}; \alpha_3 = \left(\frac{35}{f_{cm}}\right)^{0,5} \quad (15)$$

Coefficients α_1 and α_2 are meant to adjust the notional creep coefficient through the Φ_{RH} term. Coefficient α_3 is meant to be the adjustment for the time dependency function. Eqs. (4) and (9) have been rearranged in following form

$$\Phi_{RH} = \alpha_2 \left[1 + \alpha_1 \frac{1 - RH/100}{0,1 \sqrt[3]{h}}\right] \quad (16)$$

The shrinkage model represents a major change. The total shrinkage is subdivided into the autogenous shrinkage

component and the drying shrinkage component. With this approach it was possible to formulate a model which is valid for both normal strength concrete and high performance concrete having compressive strength up to 120 MPa.

The total shrinkage strain at time t is calculated as

$$\beta_H = 1,5[1 + (0,012RH)^{18}]h_0 + 250\alpha_3 \leq 1500\alpha_3 \quad (17)$$

$$\varepsilon_b^f(y) = \varepsilon_{cs}(t, t_s) = \varepsilon_{cas}(t) + \varepsilon_{cds}(t, t_s) \quad (18)$$

$$\varepsilon_{cas}(t) = \varepsilon_{cas0}(f_{cm}) \cdot \beta_{as}(t) \quad (19)$$

$$\varepsilon_{cds}(t, t_s) = \varepsilon_{cds0}(f_{cm}) \cdot \beta_{RH}(RH) \cdot \beta_{ds}(t, t_s) \quad (20)$$

Where

$\varepsilon_{cas}(t)$ and $\varepsilon_{cds}(t, t_s)$: the autogenous and drying shrinkage strain at time t , respectively;

$\varepsilon_{cas0}(f_{cm})$ and $\varepsilon_{cds0}(f_{cm})$: the notional autogenous and drying shrinkage coefficients, respectively;

$\beta_{as}(t)$ and $\beta_{ds}(t - t_s)$: the time development function for autogenous and drying shrinkage, respectively;

$\beta_{RH}(RH)$: the coefficient taking into account the effect of relative humidity on drying;

t : the concrete age in days;

t_s : the age of concrete, when drying begins in days;

The complete description of the 1999 update of the CEB-FIP MC1990 model can be found in the fib Bulletin (FIB 1999).

2.5 ACI 209 model

ACI 209 model (ACI 209 1998) recommends a procedure and set of equations for predicting creep effects in concrete structures. The method for predicting creep, established in this model, is valid for both normal and lightweight concrete, subjected to standard conditions.

The creep coefficient, under standard conditions, is expressed by

$$\Phi(t, t_0) = \frac{(t - t_0)^{0,6}}{10 + (t - t_0)^{0,6}} \Phi(t_0) \quad (21)$$

Where

t_0 : the initial time of loading in days;

t : age of concrete in days of loading (days);

$\Phi(t_0)$: the final creep coefficient and expressed as

$$\Phi(t_0) = 2,35 \prod_{i=1}^6 \gamma_{c,i} \quad (22)$$

Where $\gamma_{c,i}$, $i=1 \dots 6$ are empirical coefficients with account for parameters affecting the creep magnitude.

Coefficient $\gamma_{c,1}$ accounts the concrete age at the time of the first loading, t_0 .

$$\gamma_{c,1} = \begin{cases} 1,25 \cdot t_0^{-0,118}, & t_0 > 7 \text{ days; moist cured} \\ 1,13 \cdot t_0^{-0,094}, & t_0 > 1 - 3 \text{ days steam cured} \end{cases} \quad (23)$$

Coefficient $\gamma_{c,2}$ includes the effect of variations in the ambient relative humidity, RH (%)

$$\gamma_{c,2} = 1,27 - 0,0067 \cdot RH, \quad RH > 40\% \quad (24)$$

Coefficient $\gamma_{c,3}$ accounts the size and shape of the member. Two alternative methods are given for the

Table 2 Correction factor accounts size and shape of the member for deriving creep and shrinkage

Effects	Average thickness $h_{0,ACI}$				
	51	76	104	127	152
Creep	1,3	1,17	1,11	1,04	1,00
Shrinkage	1,35	1,25	1,17	1,08	1,00

estimation of $\gamma_{c,3}$ (ACI 209 1998). Here presented technique is based on the average thickness h_0 , $ACI=2h_0$ (see Eq. (7)) and recommended for average thicknesses up to about 305 to 380 mm. For average thickness of the member less than 150 mm, $\gamma_{c,3}$ is obtained from Table 2.

For average thickness of members greater than 150 mm and up to 380 mm, $\gamma_{c,3}$ is calculated by the equation

$$\gamma_{c,3} = \begin{cases} 1,14 - 0,00092 \cdot h_{0,ACI}; & t + t_0 \leq 1 \text{ year} \\ 1,10 - 0,00067 \cdot h_{0,ACI}; & t + t_0 > 1 \text{ year} \end{cases} \quad (25)$$

Coefficients $\gamma_{c,4} \dots \gamma_{c,6}$ depend on the composition of the concrete

$$\begin{aligned} \gamma_{c,4} &= 0,82 + 0,00264 \cdot s; \quad s > 130 \text{ mm}; \\ \gamma_{c,5} &= 0,88 + 0,0024 \cdot \theta; \quad \theta < 40 \text{ or } \theta > 60\%; \\ \gamma_{c,6} &= 0,46 + 0,09 \cdot a < 1,0; \quad a > 8\%, \end{aligned} \quad (26)$$

Where s is the slump of the fresh concrete (mm); θ -the ratio of the fine aggregate to total aggregate by weight (%) and a is the air content (%). These coefficients in undefined intervals are assumed equal to 1,0.

Under a constant stress σ_0 first applied at age t_0 , the load-dependent strain at time t is derived from the relationship

$$\varepsilon(t) = \frac{\sigma_0}{E_c(t_0)} [1 + \Phi(t, t_0)] \quad (27)$$

Where $E_c(t_0)$ is obtained from the equation presented in Table 1. The concrete strength at age t_0 may be obtained from the 28 day strength by the equation

$$f_c(t) = \frac{t_0}{\alpha + \beta \cdot t_0} f_c(28) \quad (28)$$

Where α and β depend on the cement type and curing conditions. For normal Type I cement, these coefficients are assumed equal to 4 and 0,85 (for moist curing) and 1 and 0,95 (for steam curing), respectively.

The shrinkage strain at time t measured from the start of drying is calculated by following equation

$$\varepsilon_b^f(y) = \varepsilon_{cs}(t) = \begin{cases} \varepsilon_{cs,u} t / (35 + t); & \text{moist cured} \\ \varepsilon_{cs,u} t / (55 + t); & \text{steam cured} \end{cases} \quad (29)$$

Where $\varepsilon_{cs,u}$ is the ultimate shrinkage at time infinity and represents the product of the applicable correction factors

$$\varepsilon_{cs,u} = 780 \times 10^{-6} \prod_{i=1}^7 \gamma_{cs,i} \quad (30)$$

Where $\gamma_{cs,i}$, $i=1 \dots 7$ are empirical coefficients with account for parameters affecting the shrinkage magnitude.

Coefficient $\gamma_{cs,1}$ includes the effect of variations in the ambient relative humidity, RH (%)

$$\gamma_{cs,1} = \begin{cases} 1,40 - 0,0102 \cdot RH, & 40 \leq RH \leq 80\% \\ 3,00 - 0,0030 \cdot RH, & 80 \leq RH \leq 100\% \end{cases} \quad (31)$$

Coefficient $\gamma_{cs,2}$ accounts for the size and shape of the

Table 3 Shrinkage correction factor accounts for initial moist curing period

Curing period in days	1	3	7	14	28	90
$\gamma_{c,7}$	1,2	1,1	1,0	0,93	0,86	0,75

member. Two alternative methods as in creep analysis are given in (ACI 209 1998) for estimating the $\gamma_{cs,2}$. Herein presented technique is based on the average thickness $h_{0,ACI}$ (Table 2).

For average thickness of members greater than 150 mm and up to 380 mm, $\gamma_{cs,2}$ is calculated using the equation

$$\gamma_{cs,2} = \begin{cases} 1,23 - 0,0015 \cdot h_{0,ACI}; & t - t_0 \leq 1 \text{ year} \\ 1,17 - 0,0011 \cdot h_{0,ACI}; & t - t_0 > 1 \text{ year} \end{cases} \quad (32)$$

Coefficients $\gamma_{cs,3} \dots \gamma_{cs,7}$ depend on the composition of the concrete

$$\begin{aligned} \gamma_{cs,3} &= 0,89 + 0,00161 \cdot s; \quad s > 130 \text{ mm}; \\ \gamma_{cs,4} &= \begin{cases} 0,30 + 0,014 \cdot \psi; & \psi \leq 50\% \\ 0,90 + 0,002 \cdot \psi; & \psi > 50\% \end{cases} \\ \gamma_{cs,5} &= 0,95 + 0,008 \cdot \alpha; \quad \alpha > 8\% \\ \gamma_{cs,6} &= 0,75 + 0,00061 \cdot c, \end{aligned} \quad (33)$$

Where c is cement content in concrete (kg/m^3); other parameters are analogous to Eq. (26). These coefficients in undefined intervals are assumed equal to 1,0.

Coefficient $\gamma_{cs,7}$ accounts for variations in the period of initial moist curing and is presented in Table 3. For a concrete which is steam cured for a period of between one and three days $\gamma_{cs,7}=1,0$.

2.6 Bazant & Baweia (B3) model

The complete description of the B3 model can be found in (Bazant et al. 1995a, Bazant et al. 1995b).

The mean shrinkage strain at time t is given as

$$\varepsilon_b^f(y) = \varepsilon_{cs}(t, t_0) = \varepsilon_{cs\infty} k_{RH} S(t) \quad (34)$$

Where

$$\varepsilon_{cs\infty} = \alpha_1 \alpha_2 (1,9 \times 10^{-2} W^{2,1} f_{cm}^{-0,28} + 270) \times 10^{-6} \quad (35)$$

$$S(t) = \tanh \sqrt{(t - t_0) / \tau_{sh}} \quad (36)$$

Where

$\varepsilon_{cs\infty}$: the ultimate shrinkage;

$S(t)$: the time function for shrinkage;

α_1 and α_2 : the correlation terms for effects of cement type and curing conditions respectively;

W : the water content;

k_{RH} : humidity dependence factor;

t : the age of concrete;

t_0 : the age, when during begins;

τ_{sh} : the size dependence factor.

The B3 model takes into account the influence of the material composition directly. Besides model parameters, which are considered in previously reviewed models, the cement content, the water-cement ratio, the aggregate-cement ratio and the water content are taken into account.

The prediction model parameters and corresponding

Table 4 Models variables and limitations

Variable	CEB-FIP MC 90 Model	ACI 209 Model	Bazant & Baweja (B3) Model
f_{cm} (MPa)	20-120	----	17-69
A/C	----	----	2,5-13,5
Cement (kg/m ³)	----	----	160-720
W/C	----	----	0,35-0,85
RH (%)	40-100	40-100	40-100
Cement type	I, II or III	I, II or III	I, II or III
t_o or t_s (moist cured)	----	≥ 7 days	$t_s \leq t_o$
t_o or t_s (steam cured)	----	$\geq 1-3$ days	$t_s \leq t_o$

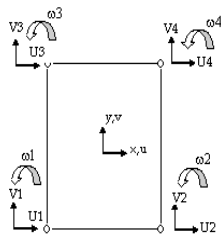


Fig. 1 Cheung's type element (12 DOFs)

limitations for the CEB-FIP MC 90, ACI 209 and B3 models are presented in Table 4. In this table, A/C is aggregate-to-cement ratio; W/C is water-to-cement ratio, t_o and t_s are the age of concrete at loading and beginning of a shrinkage, respectively.

3. Finite element model for reinforced shear walls

The finite element method (FEM) is a generalization of standard structural analysis procedures which permit the calculation of stresses and deflections in two and three dimensional structures. It has been popular for many years to analyze any type of building structures. However, due to relatively low efficiency and high computing cost, it has never been popular for shear walls analysis. The experiences with this method revealed that some applications are not as straightforward as initially conceived. Particularly, it has been found that many lower-order elements such as the bilinear elements are subjected to parasitic shear, which greatly stiffens the elements in their response to bending. Also, it is felt that the best method of dealing with parasitic shear is to avoid them by using elements that can exactly represent the strain state of pure bending.

To obtain an improved element, Cheung *et al.* (1978) and Chan *et al.* (1979) were developed the finite strip element, and higher order element to modelize the shear wall with the rotational DOFs for representing the strain state of pure bending.

Cheung (1983) and Lee (1987) provided a 12 DOFs plane stress element having two translational DOFs and one DOF per node (Fig. 1). Their works have been used in many researches (Kim *et al.* 2003). As suggested by Kwan (1992, 1993), by neglecting the lateral strain in the wall,

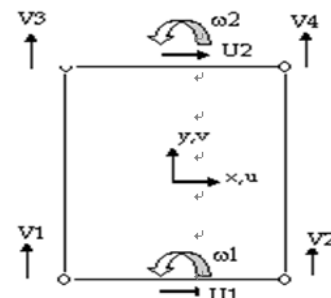


Fig. 2 Kwan's strain based element (8 DOFs)

which are generally of little significance. The DOFs can be reduced from 12 to 8 as shown in Fig. 2. Use of this simplified Cheung's element, which is computationally more efficient, is recommended rather the original Cheung's element. Using the mixed FEM, Kwan (1992) developed a wall element with the 8 DOFs. This element included two existing elements, namely the simplified Cheung's element (Cheung 1983) and Kwan's strain based element (1993).

4. Solution procedure

4.1 Creep and shrinkage effect on the elastic deformation of RC shear walls

The strain $\varepsilon_b(y)$ in the RC shear walls can be expressed as

$$\varepsilon_b(y) = \varepsilon(y) + \varepsilon_b^f(y) \quad (37)$$

Where $\varepsilon(y)$ is the vertical strain of RC shear walls which is expressed as

$$\varepsilon(y) = \frac{dv}{dy} \quad (38)$$

4.2 Fibre volume fraction V_f

The plates are made of fibre composite with varying fibre volume fraction widthwise (Kubiak 2005). Widthwise variable of fibre volume fraction V_f was assumed as sinusoid function in the following way

$$V_f = V_{fav} + A_i \cdot \cos\left(\frac{2\pi x}{b}\right) \quad (39)$$

Where $V_{fav}=0.5$ is the assumed average value for fibre volume fraction, A_i is the sinusoid amplitude defining variation of material properties widthwise plate, with a calculated range of amplitude from -0.4 to 0.4 and b is width of the plate. In order to determine the magnitude characterising material properties, Eq. (40) found in literature (Kelly 1989) were used basing on theory of mixture.

Using Eq. (40) it is possible to determine an equivalent value for the following material properties:

- Modulus of elasticity in transverse direction E_y ,
- Shear modulus G_{xy} ,
- Poisson ratio ν_{xy} .

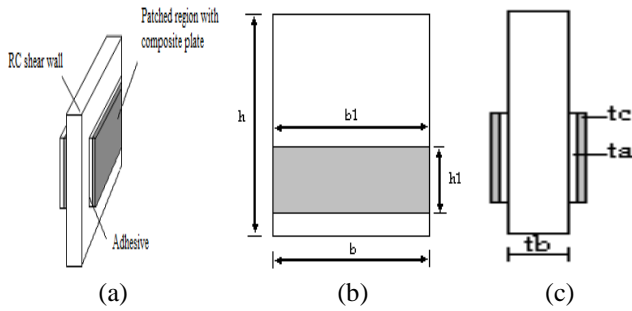


Fig. 3 A strengthened RC shear wall: (a) perspective view; (b) front view and (c) lateral view

$$E_y = E_m \cdot \frac{E_m \cdot (1 - \sqrt{V_f}) + E_f \cdot \sqrt{V_f}}{E_m \cdot [1 - \sqrt{V_f} \cdot (1 - \sqrt{V_f})] + E_f \cdot \sqrt{V_f} \cdot (1 - \sqrt{V_f})}$$

$$G_{xy} = G_m \cdot \frac{G_m \sqrt{V_f} (1 - \sqrt{V_f}) + G_f \cdot [1 - \sqrt{V_f} (1 - \sqrt{V_f})]}{G_m \cdot \sqrt{V_f} + G_f \cdot (1 - \sqrt{V_f})} \quad (40)$$

$$v_{xy} = v_m \cdot (1 - \sqrt{V_f}) + v_f \cdot \sqrt{V_f}$$

4.3 Stiffness matrix of the shear wall element

Figs. 3(a), (b) and (c) describe a combination of composite plates having variable fibre volume fraction widthwise and a reinforced shear wall, attached to the two sides using adhesive plates. The adhesives are assumed to be isotropic shear walls of thickness t_a , the external adherents are considered to be composite shear walls of thickness t_c bonded to the area $S_B = bh_1$. In the static analysis problem, the shear wall element which has the total area $S_T = bh$ is subjected to lateral load. Let us denote by μ the deflection, v the vertical displacement and ω the rotation of the vertical fibers.

The mixed finite element method established by Kwan (1992) was deployed to deduce the stiffness matrix of a proposed strengthened shear wall system. The displacement components at any point within the wall element may be expressed in the terms of the nodal DOF of the element as follows

$$u = u_1 \cdot \left(\frac{1}{2} - \frac{3}{2} \left(\frac{y}{h} \right) + 2 \cdot \left(\frac{y}{h} \right)^3 \right) + \omega_1 h \cdot \left(-\frac{1}{8} + \frac{1}{4} \cdot \left(\frac{y}{h} \right) + \frac{1}{2} \cdot \left(\frac{y}{h} \right)^2 - \left(\frac{y}{h} \right)^3 \right) + u_2 \cdot \left(\frac{1}{2} + \frac{3}{2} \left(\frac{y}{h} \right) - 2 \cdot \left(\frac{y}{h} \right)^3 \right) + \omega_2 h \cdot \left(\frac{1}{8} + \frac{1}{4} \cdot \left(\frac{y}{h} \right) - \frac{1}{2} \cdot \left(\frac{y}{h} \right)^2 - \left(\frac{y}{h} \right)^3 \right) \quad (41)$$

$$v = v_1 \cdot \left(\frac{1}{2} - \frac{x}{b} \right) \cdot \left(\frac{1}{2} - \frac{y}{h} \right) + v_2 \cdot \left(\frac{1}{2} + \frac{x}{b} \right) \cdot \left(\frac{1}{2} - \frac{y}{h} \right) + v_3 \cdot \left(\frac{1}{2} - \frac{x}{b} \right) \cdot \left(\frac{1}{2} + \frac{y}{h} \right) + v_4 \cdot \left(\frac{1}{2} + \frac{x}{b} \right) \cdot \left(\frac{1}{2} + \frac{y}{h} \right) + \left(\frac{6}{h} \cdot (u_1 - u_2) - 3 \cdot (\omega_1 + \omega_2) \right) \cdot \left(\frac{1}{4} - \left(\frac{y}{h} \right)^2 \right) \cdot \left(\frac{x}{2} + \frac{b}{4} \right) \quad (42)$$

The strain energy for each wall element can be written as

$$U^e = U_B^e + U_S^e \quad (43)$$

Where: U_B^e and U_S^e are the strain energy due to the bending and shear effects respectively, which are written as e function of the strains on the shear wall element. The strain energy considering only the bending effect U_B^e is done as

$$U_B^e = \frac{1}{2} \sum_{i=1}^3 \int E_y^{(i)} (\varepsilon_b(y))^2 dx dy dz \quad (44)$$

According to this relationship, the strain energy U_B^e can be expressed as

$$U_B^e = \frac{1}{2} \left[\begin{aligned} & E_{bt}^{(1)} t_b \int_{-\frac{h}{2}}^{\frac{h}{2}} \int_{-\frac{b}{2}}^{\frac{b}{2}} (\varepsilon_b(y))^2 dx dy + \\ & 2E_a^{(2)} t_a \int_{y_1 - \frac{h_1}{2}}^{y_1 + \frac{h_1}{2}} \int_{-\frac{b}{2}}^{\frac{b}{2}} (\varepsilon(y))^2 dx dy + \\ & 2t_c \int_{y_1 - \frac{h_1}{2}}^{y_1 + \frac{h_1}{2}} \int_{-\frac{b}{2}}^{\frac{b}{2}} E_y (\varepsilon(y))^2 dx dy \end{aligned} \right] \quad (45)$$

The expression of the strain energy which relate to the shear effect may be written as

$$U_S^e = \frac{1}{2} \sum_{i=1}^3 \int G_{xy}^{(i)} (\gamma(xy))^2 dx dy dz \quad (46)$$

The insertion of this relationship into the previous equation leads to the following expression

$$U_S^e = \frac{1}{2} \left[\begin{aligned} & G_{bt}^{(1)} t_b \int_{-\frac{h}{2}}^{\frac{h}{2}} \int_{-\frac{b}{2}}^{\frac{b}{2}} (\gamma(xy))^2 dx dy + \\ & 2G_a^{(2)} t_a \int_{y_1 - \frac{h_1}{2}}^{y_1 + \frac{h_1}{2}} \int_{-\frac{b}{2}}^{\frac{b}{2}} (\gamma(xy))^2 dx dy + \\ & 2t_c \int_{y_1 - \frac{h_1}{2}}^{y_1 + \frac{h_1}{2}} \int_{-\frac{b}{2}}^{\frac{b}{2}} G_{xy} (\gamma(xy))^2 dx dy \end{aligned} \right] \quad (47)$$

In which

$$\gamma(xy) = \frac{dv}{dx} + \frac{du}{dy} \quad (44)$$

The following form of the strain energy for each wall element is expressed by

$$U^e = \frac{1}{2} d_e^T K_w d_e \quad (49)$$

Where the nodal displacement vector is given as $d_e^T = \{u_1, \omega_1, v_1, v_2, u_2, \omega_2, v_3, v_4\}$. To carry out numerical analysis, we employ the standard finite element formulation to determine the stiffness matrix K_w of a strengthened shear wall element. No explicit procedure to determine the stiffness matrix needs to be given here. However, more detailed information can be found in reference (Bathe 1996).

4.4 System equation of motion

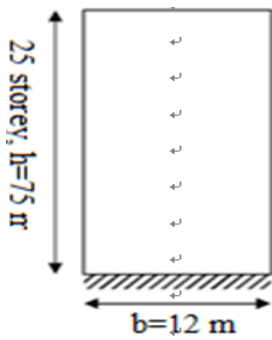


Fig. 4 Shear walls structures: 25 storey

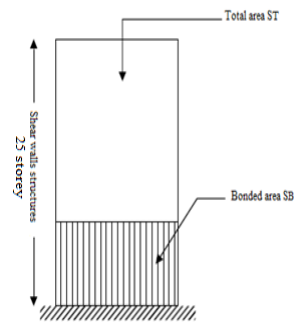


Fig. 5 Externally bonded plates at the base of shear walls structures (25 storey)

The generalized differential equation of motion for the coupled shear walls may be expressed as

$$[M].\ddot{D}(t) + [C].\dot{D}(t) + [K].D(t) = -[M].E.D\ddot{g}(t) \quad (50)$$

In which $[C]$ and $[K]$ are the global damping and stiffness matrices of the structures, respectively, $D(t)$, $\dot{D}(t)$ and $\ddot{D}(t)$ are the relative displacement, velocity and acceleration vectors to the structures with respect to base; E is a location vector which defines the location of effective seismic loads and $\ddot{D}_g(t)$ is the horizontal ground acceleration.

The damping matrix of the model is assumed to be proportional to the stiffness and mass matrices by the Rayleigh's proportionality factors α_1 , α_2 and can be written as

$$[C] = \alpha_1.[M] + \alpha_2.[K] \quad (51)$$

The proportionality factors α_1 , α_2 can be obtained from

$$\alpha_1 = \xi \cdot \frac{2\lambda_j\lambda_p}{\lambda_j + \lambda_p} \text{ and } \alpha_2 = \xi \cdot \frac{2}{\lambda_j + \lambda_p} \quad (52)$$

Where λ_j and λ_p are two chosen natural frequencies of the shear wall structures, which are determined by solving the undamped eigenvalue equation

$$|[K] - \lambda^2[M]| = 0 \quad (53)$$

ξ is the assumed damping ratio for the two chosen modes. In the present analysis, the damping ratio is taken as 5%. The Newmark- β step-by-step time-integration method is employed to obtain the solution of the dynamic equation. The two parameter β and γ of the Newmark integration are taken as $\frac{1}{4}$ and $\frac{1}{2}$ respectively. To achieve a reasonable accuracy of the dynamic response of the structure, the time step is made sufficiently small compared with the periods of the first few modes of vibration of the structure.

5. Numerical study

In order to verify the accuracy of the mechanical concept of the proposed method, a typical 25 storey shear wall structures is analyzed. The shear wall is strengthened by bonded CFRP plates, at the bottom (see Figs. 4 and 5).

Table 5 Mechanical properties of materials

Materials	Concrete	Adhesive epoxy	Carbon
Modulus of elasticity E (GPa)	---	3	3,445
Poisson's ratio ν	0.18	0.35	0.22

Table 6 Dimensions properties of shear walls structure

Shear walls structures	Dimensions			
	TH (m)	SH (m)	WW(m)	WT (m)
25 storey	75	3	12	0.25

TH: Total Height; SH: Storey Height; WW: Wall Width; WT: Wall Thickness

Table 7 Properties of earthquake records

Earthquake	Site	Date	Ground acceleration max	Magnitude
El-Asnam	Site	10-10-1980	0.049 g	7.3
Boumerdés	Boumerdés: Keddara	21-05-2003	0.35 g	6.8

On the basis of the presented analysis method, to demonstrate the effect of creep and shrinkage on the earthquake response of RC shear walls, the following data have been used for the numerical results: RH=40%, $t_0=28$ days, $t=120$ days. The numerical values of the geometry and materials properties for shear walls structure are summarized in Tables 5 and 6. Also, one material for strengthening is investigated, consisting of carbon fibres with an epoxy matrix. Their material properties are given in Table 5.

5.1 Earthquake records

In general, earthquakes have different properties, such as peak acceleration, duration of strong motion and different ranges of dominant frequencies, and therefore have different influences on the structure. Two earthquake excitations are used in this study. El Asnam and Boumerdes earthquake records (see Table 7) were selected to investigate the dynamic response of the structure.

5.2 Time-dependent analysis of eigenfrequencies

An RC shear wall structures strengthened with composite plates having the fiber distribution $V_f=0.9$ is being considered. On the basis of the presented numerical method, a computer program has been written for 25 storey shear wall structures in order to evaluate the influence of creep and shrinkage on the three firsts eigenfrequencies of RC shear wall structures strengthened by CFRP. The structure strengthened is subjected to Boumerdes earthquake. The results are presented on Tables 8 and 9.

We denote by: CEB-FIP MC 90 model: model I, ACI 209 model: model II and Bazant & Baweja (B3) model: model III.

Tables 8 and 9 show the creep and shrinkage effect on

Table 8 Three firsts frequencies (Hz), bonded plates at the base with: 25 storey structure, $t=120$ days, $RH=40\%$, $t_c=0.006$ m, $S_B/S_T=20\%$, CFRP

Fibre volume Fraction V_f	Code type Model	Mode 1	Mode 2	Mode 3
$V_f = 0.5 - 0.4 \cdot \cos\left(\frac{2\pi x}{b}\right)$ (near the edge of the plate)	Model I	0.472	2.332	3.865
	Model II	0.455	2.292	3.646
	Model III	0.421	2.198	3.387
Unstrengthened model				
	Model I	0.402	2.107	3.247
	Model II	0.382	1.903	3.002
	Model III	0.348	1.772	2.872

Table 9 Three firsts frequencies (Hz), bonded plates at the base with: 25 storey structure, $RH=40\%$, $t_c=0.006$ m, $S_B/S_T=20\%$, $V_f = 0.5 - 0.4 \cdot \cos\left(\frac{2\pi x}{b}\right)$, CFRP

t (days)	Code type Model	Mode 1	Mode 2	Mode 3
120	Strengthened	0.472	2.332	3.865
	Unstrengthened	0.402	2.107	3.247
1000	Strengthened	0.455	2.292	3.646
	Unstrengthened	0.382	1.903	3.002
3000	Strengthened	0.421	2.198	3.387
	Unstrengthened	0.348	1.772	2.872
4000	Strengthened	0.456	2.317	3.782
	Unstrengthened	0.381	1.896	2.915
5000	Strengthened	0.439	2.279	3.498
	Unstrengthened	0.342	1.791	2.715
5000	Strengthened	0.411	2.187	3.209
	Unstrengthened	0.301	1.608	2.497
5000	Strengthened	0.433	2.292	3.731
	Unstrengthened	0.367	1.803	2.815
5000	Strengthened	0.418	2.263	3.424
	Unstrengthened	0.323	1.623	2.678
5000	Strengthened	0.406	2.178	3.196
	Unstrengthened	0.291	1.548	2.417
5000	Strengthened	0.427	2.266	3.715
	Unstrengthened	0.324	1.778	2.802
5000	Strengthened	0.402	2.237	3.367
	Unstrengthened	0.296	1.753	2.489
5000	Strengthened	0.383	2.171	3.046
	Unstrengthened	0.278	1.513	2.351
5000	Strengthened	0.393	2.161	3.702
	Unstrengthened	0.311	1.722	2.784
5000	Strengthened	0.364	2.117	3.309
	Unstrengthened	0.286	1.702	2.418
5000	Strengthened	0.327	2.107	2.965
	Unstrengthened	0.254	1.482	2.321

Table 10 Fibres volume fractions

The sinusoid amplitude A_i	-0.4	-0.3	-0.2	-0.1	0	0.1	0.2	0.3	0.4
Fibres volume fractions $V_f; V_{f_{av}}=0.5$	0.9	0.8	0.7	0.6	0.5	0.4	0.3	0.2	0.1

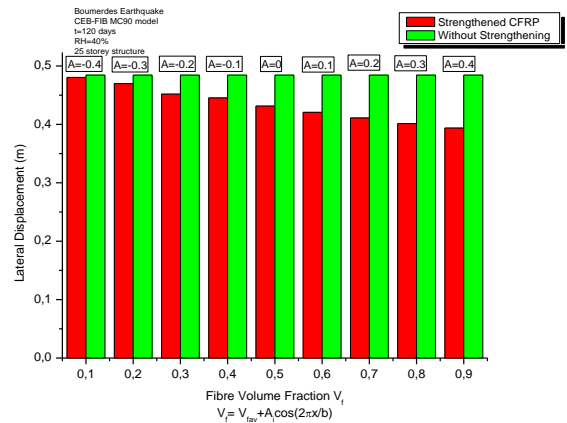
the three firsts eigenfrequencies. From table 8, it is worth noting that the values of frequencies obtained increase in comparison with unstrengthened model, under all type code models: CEB-FIP MC 90 model, ACI 209 model and Bazant & Baweja (B3) model. Also, it can be shown that model I gives higher values of frequencies comparing them with models II and III. From Table 9, increasing the age of concrete leads to decreases eigenfrequencies of RC shear wall structures, which due to the predominant action of creep and shrinkage.

The creep and shrinkage affects the modulus of elasticity of concrete and therefore on its rigidity (decrease of modulus of elasticity=decrease of stiffness) which contributes to increase the periods.

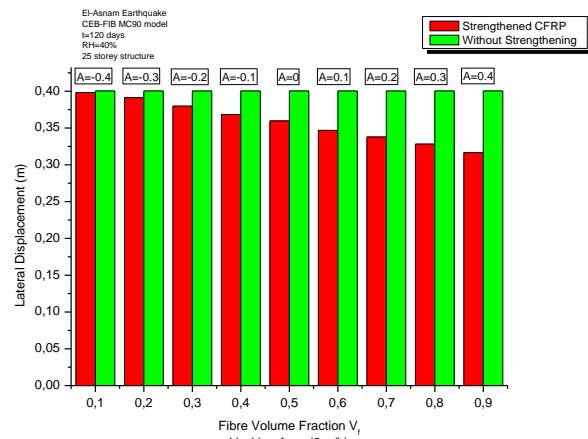
Finally, the reduction of eigenfrequencies of RC shear wall structures strengthened by CFRP plates, under all type code models, is the result of the reduction of stiffness who is lost by the creep of concrete.

5.3 Effect of widthwise varying fibre volume fraction on lateral displacement

A different distributions of fibres were considered, each characterized by variations of the amplitude A_i of sinusoidal fibres volume fraction V_f , as given in Table 10. As can be seen from Table 10, that the increase of amplitude A_i



(a) Boumerdes earthquake



(b) El Asnam earthquake

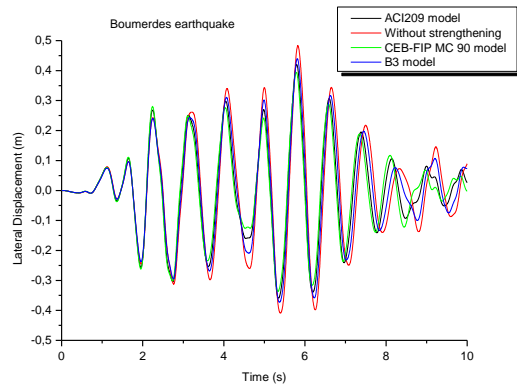
Fig. 6 Effect of widthwise varying fibre volume fraction on the top lateral displacement

from 0 to 0.4 corresponds to the increase of fibre volume fraction near the middle part of the plate and the decrease of amplitude A_i from 0 to 0.4 corresponds to the increase of fibre volume fraction near the edge of the plate.

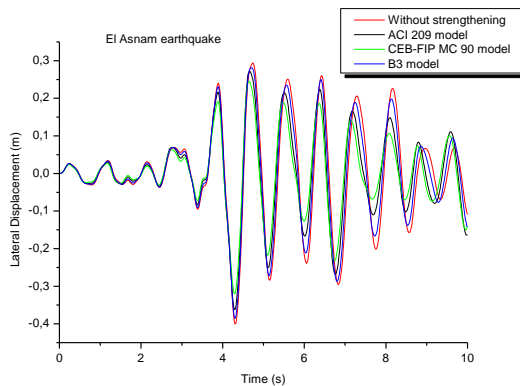
The lateral displacements at the top of RC shear walls, strengthened by composite plates having a sinusoidal variation of fibres, are presented by Figs. 6(a)-(b). The purpose of this study is to illustrate how the fibre volume fractions, with amplitude A_i of sinusoid changing from -0.4 to 0.4, affect the top lateral displacements after strengthening.

The model of a strengthened shear wall is compared with a model of reference (without strengthening), under the two selected earthquakes (El-Asnam and Boumerdes), taking into account the aging effect of concrete, mainly creep and shrinkage cited in CEB-FIP MC90 model. The lateral displacements of repaired shear wall are given by Figs. 6(a)-(b).

From the obtained results, the fact that can be concluded is that an increase in volume fraction of fibres results in an increase of Young's modulus and therefore causes decreases in the lateral displacement (lateral stiffness). The reduction has been achieved by the $V_f=0.9$ distribution with an average reduction of 18.72% for 25 storey building strengthened by CFRP plates (under



(a) Boumerdes earthquake



(b) El Asnam earthquake

Fig. 7 Time history response of the lateral displacement of strengthened shear walls structures under different “code type” models

Boumerdes earthquake). Thus, fibres must be concentrated at the edges of the composite plates where the stresses are the highest. In term of information from the location of the bonded area and the effect of the thickness of the bonded composite plates, it can be found in reference (Meftah *et al.* 2008).

5.4 Time history response of the lateral displacement of strengthened shear walls structures: Comparison from different “code type” models

The results of the time history response of the lateral displacement for the strengthened shear walls under all code type models tested in this study (CEB-FIP MC 90 model, ACI 209 model and Bazant & Baweja (B3) model), under each of the two earthquake records are presented below. An RC shear walls strengthened with composite plates having the fiber distribution $V_f=0.9$ is being considered. On the basis of the presented numerical method, a computer program has been written for 25 storey shear walls structures, in order to evaluate the influence of creep and shrinkage on the lateral displacement. The results are reported in Figs. 7(a)-(b).

Figs. 7(a)-(b) show the time history response of the lateral displacement of strengthened shear walls structures under different “code type” models. From the results, the significantly best performance has been achieved for CEB-FIP MC 90 model compared with ACI

209 model and Bazant & Baweja model.

6. Conclusions

The seismic analysis of reinforced concrete shear walls structures strengthened with composite plates having variable fibre volume fraction, including the considerations of the rheological properties of concrete mainly creep and shrinkage has been studied. It should be emphasized that the results presented in this paper are only partial, and a more detailed evaluation remains to be finished. The analysis is based on the finite element method. The following conclusions are extracted from the current study:

(a) The influence of creep on time dependent behavior of shear walls structures strengthened by CFRP sheets according to CEB-FIP MC 90 model, in comparison with ACI 209 model and Bazant & Baweja (B3) model is noted.

(b) From this study of the CEB-FIP MC 90, ACI 209 and Bazant & Baweja prediction models, it has been concluded that certain parameters have a much influence on the time-dependent response of shear walls structures strengthened.

(c) The proposed model permits the study of lateral stiffness and vibration characteristics including the opposed effects of creep and shrinkage cited in the three code type models.

(d) Significant improvement in the displacements was observed when the fibers are clustering near the wall edges, so that they are concentrated.

(e) The evaluated frequencies modes are decreased with time also due to the action of creep and shrinkage.

(f) The influence of creep action is more significant in the early ageing of concrete.

(g) The creep and shrinkage effect must be carefully evaluated in order to understand the behavior of shear walls structures repaired by CFRP.

(h) Analysis results show that the application of externally bonded carbon fiber sheets is an effective seismic strengthening procedure for RC shear walls.

Acknowledgments

The authors would like to thank the anonymous referees for improving the quality of this manuscript and for their valuable comments.

References

- ACI committee 209 (1998), *Prediction of Creep, Shrinkage and Temperature Effects in Concrete Structures*.
- Al-Manasseer, A. and Lam, J.P. (2005), “Statistical evaluation of shrinkage and creep models”, *ACI Mater. J.*, **102**(3), 170-176.
- Almeida, L.C. (2006), “Identificação de parâmetros estruturais com emprego de análise inversa”, Campinas, Tese (Doutorado), Faculdade de Engenharia Civil, Arquitetura e Urbanismo da Universidade Estadual de Campinas, 192.

- Bathe, K.J. (1996), *Finite Element Procedures*, Prentice Hall Inc., New Jersey, U.S.A.
- Bazant, Z.P. and Baweja, S. (1995a), "Justification and refinements of model B3 for concrete creep and shrinkage: Statistics and sensitivity", *Mater. Struct.*, **28**(7), 415-430.
- Bazant, Z.P. and Baweja, S. (1995b), "Justification and refinements of model b3 for concrete creep and shrinkage: Updating and theoretical basis", *Mater. Struct.*, **28**(8), 488-495.
- Boukhezar, M., Samai, M.L., Mesbah, H.A. and Houari, H. (2013), "Flexural behaviour of reinforced low-strength concrete beams strengthened with CFRP plates", *J. Struct. Eng. Mech.*, **47**(6), 819-838.
- Chan, H.C. and Cheung, Y.K. (1979), "Analysis of shear walls using higher order element", *J. Build. Environ.*, **14**(3), 217-221.
- Cheung, Y.K. (1983), *Tall Building 2, Handbook of Structural Concrete*, Pitman Books Limited, London, U.K.
- Cheung, Y.K. and Swaddiwudhipong, S. (1978), "Analysis of shear wall structures using finite strip elements", *Proceedings of the Institution of Civil Engineers*, London, U.K.
- Chia, K.S., Liu, X., Liew, J.Y.R. and Zhang, M.H. (2014), "Experimental study on creep and shrinkage of high-performance ultra light weight cement composite of 60 MPa", *J. Struct. Eng. Mech.*, **50**(5), 635-652.
- Chung, L., Park, T.W. and Hwang, J.H. (2014), "Strengthening methods for existing wall type structures by installing additional shear walls", *J. Struct. Eng. Mech.*, **49**(4), 523-536.
- Comité Euro-International du Béton (1991), *CEB-FIP Model Code 1990/Design Code*, Thomas Telford.
- Comité Européen de Normalisation du Béton (2001), *Design of Concrete Structures-Part 1: General Rules and Rules of Building*, Eurocode, Brussels, Belgium.
- Federation Internationale du Béton (1999), *Textbook on Behavior, Design and Performance*, Updated Knowledge of the CEB Model Code, Structural Concrete.
- Kelly, A. (1989), *Concise Encyclopedia of Composite Materials*, Pergamon Press.
- Kim, H.S. and Lee, D.G. (2003), "Analysis of shear wall with openings using super elements", *J. Eng. Struct.*, **25**(8), 981-991.
- Kubiak, T. (2005), "Dynamic buckling of thin-walled composite plates with varying widthwise material properties", *J. Sol. Struct.*, **42**(20), 5555-5567.
- Kwan, A.K.H. (1992), "Analysis of building used strain based element with rotational DOF", *J. Struct. Eng.*, **118**(5), 1191-1121.
- Kwan, A.K.H. (1993), "Mixed finite element method for analysis of coupled shear/core", *J. Struct. Eng.*, **119**(5), 1388-1401.
- Lee, D.G. (1987), "An efficient element for analysis of frames with shear walls", *ICES88*, Atlanta, U.S.A.
- Meftah, S.A., Yeghnem, R., Tounsi, A. and Adda Bedia, E.A. (2008), "Lateral stiffness and vibration characteristics of composites plated RC shear walls with variable fibres spacing", *J. Mater. Des.*, **29**(10), 1955-1964.
- Meyerson, R., Weyers, R.E., Mokarem, D.W. and Lane, D.S. (2002), "Evaluation of models for predicting (total) creep of prestressed concrete mixtures", Final Contract Report VTRC 03-CR5, Virginia, U.S.A.
- Mini, K.M., Alpat, R.J., David, A.E., Radhakrishnan, A., Cyriac, M.M. and Ramakrishnan, R. (2014), "Experimental study on strengthening of R.C. beam using glass fibre reinforced composite", *J. Struct. Eng. Mech.*, **50**(3), 275-286.
- Sakr, M.A., El-Khoriby, S.R., Khalifa, T.R. and Nagib, M.T. (2017), "Modeling of RC shear walls strengthened by FRP composites", *J. Struct. Eng. Mech.*, **61**(3), 407-417.
- Takács, P.F. (2002), "Deformations in concrete cantilever bridges: Observations and theoretical modelling", Ph.D. Dissertation, The Norwegian University of Science and Technology, Trondheim, Norway.
- Wang, Q., Chai, Z. and Wang, L. (2014), "Seismic capacity of brick masonry walls externally bonded GFRP under in-plane loading", *J. Struct. Eng. Mech.*, **51**(3), 413-431.
- Yeghnem, R., Boulefrakh, L., Meftah, S.A., Tounsi, A., Adda Bedia, E.A. (2015), "Time dependent behavior of damaged reinforced concrete shear walls strengthened with composite plates having variable fibers spacing", *J. Civil Environ. Struct. Constr. Architect. Eng.*, **9**(12), 1484-1488.
- Yeghnem, R., Meftah, S.A., Tounsi, A. and AddaBedia, E.A. (2009), "Earthquake response of RC coupled shear walls strengthened with thin composite plates", *J. Vibr. Contr.*, **15**(7), 963-985.

CC